Petrology and deformation history of the metamorphic basement in the Mezősas-Furta crystalline high (SE Hungary)

Tivadar M. Tóth, Judit Zachar
Department of Mineralogy, Geochemistry and Petrology,
University of Szeged, Szeged

The metamorphic basement of the Pannonian Basin consists of uplifted highs and deep sub-basins among them. One of the best-known highs is the so-called Szeghalom Dome, which is surrounded by less intensely explored ones. The eastern neighbour, the Mezősas-Furta Dome (MFD), is studied in this paper.

Based on detailed petrologic investigation, six main lithologies are distinguished for the MFD, which can be well compared to those described previously for the Szeghalom Dome. All these rock types (orthogneiss, mafic-ultramafic xenolith, granite, sillimanite-biotite gneiss, garnet-bearing amphibolite, amphibole-biotite gneiss) are classified into three main units based on different metamorphic and deformation history. Understanding their relative spatial position permitted the elaboration of geologic map and sections of the MFD.

Key words: Pannonian Basin, metamorphic basement, orthogneiss, xenolith, deformation history

Introduction

The basement of the Pannonian Basin north of the Békés Basin forms a series of uplifted metamorphic domes. The best explored among them is the Szeghalom Dome, which has been studied previously from several aspects. The evolution scheme, and the database behind it, provides sufficient information for comparison with the structure and evolution of the neighbouring domes, which otherwise supply less information because of the small amount of available core material. In this paper, rock types of the eastern neighbour, the Mezősas-Furta Dome, are presented. We aim to classify them so that, as far as possible, the rock

classes are comparable to those described in the case of the Szeghalom Dome. Since the structure and the evolution of the metamorphic basement of the Pannonian Basin is rather complicated, a consistent geologic model can be framed only if as many petrologic and microstructural data as possible are involved in the same model. We aim to sketch a reliable spatial model of the relative position of the blocks of homogeneous evolution, taking into account data for both the Szeghalom and the Mezősas-Furta Domes.

Geologic setting

The Mezősas-Furta Dome (MFD) belongs to the series of the metamorphic highs limiting the Békés Basin in the north. To the west, it is bordered by the relatively well-known Szeghalom Dome (SzD), and further westward follow the Déva, Endrőd and Szarvas Domes (Fig. 1). One of the best documented among the crystalline highs is the Szeghalom Dome (M. Tóth et al. 2000; Schubert et al. 2001; Schubert and M. Tóth 2001; Zachar and M. Tóth 2001; Juhász et al. 2002; M. Tóth et al. 2003a, b; Schubert and M. Tóth 2003). There are data concerning the lithological framework of the dome suggesting the presence of four blocks, which became juxtaposed through post-metamorphic movements (M. Tóth et al. 2000). In the central range of the dome the lowermost unit consists essentially of a homogeneous paragneiss unit. Depending on the chemical composition, the rock samples may contain sillimanite, and in places traces of a low degree partial melting is also observable. Biotite-garnet thermometer (Ferry and Spear 1978) suggests T_{max} in the range of 650–700 °C. In the deepest position, either within or beneath the sillimanite-bearing paragneiss unit, metabasic rock samples appear, which exhibit textural relics of an early high-pressure evolution. Thermo-barometric calculations result in a peak condition of about 600–650 °C and >12 kbar (M. Tóth 1997). It is still under debate whether the eclogite cores represent an independent unit below the paragneiss, or they form xenoliths in the gneiss itself. The topmost segment of the basement overlies a thick cataclasite zone. Here amphibolite, amphibole-biotite gneiss and biotite gneiss are the characteristic rock types, all suggesting a T_{max} value < 600 °C. Geochemically, amphibolite represents a back-arc basin tholeiite (M. Tóth 1994a), different samples exhibiting different state of igneous differentiation. The northern slope of the dome exhibits a significantly different lithology. Here a monotonous orthogneiss unit reigns, and all the previous rock types are absolutely unknown. The orthogneiss body is crosscut by a small number of microgranite dykes. The igneous origin of the gneiss is obvious because of the presence of the numerous idiomorphic accessory mineral grains (zircon and apatite), myrmekitic plagioclase grains (Zachar and M. Tóth 2001), as well as relic polygonal quartz–feldspar textures. Following the thermal peak, the orthogneiss body formed mylonite along a wide shear zone under greenschist facies conditions (Schubert and M. Tóth 2001).

Fig. 1
Topographic map of the Pre-Neogene basement of the eastern part of the Pannonian Basin. Isolines denote depth below the present surface. Inset: Location of the study area in the Alpine–Carpathian–Pannonian System. A – Alps, BM – Bohemian Massif, C – Carpathians, D – Dinarides, PB – Pannoonian Basin
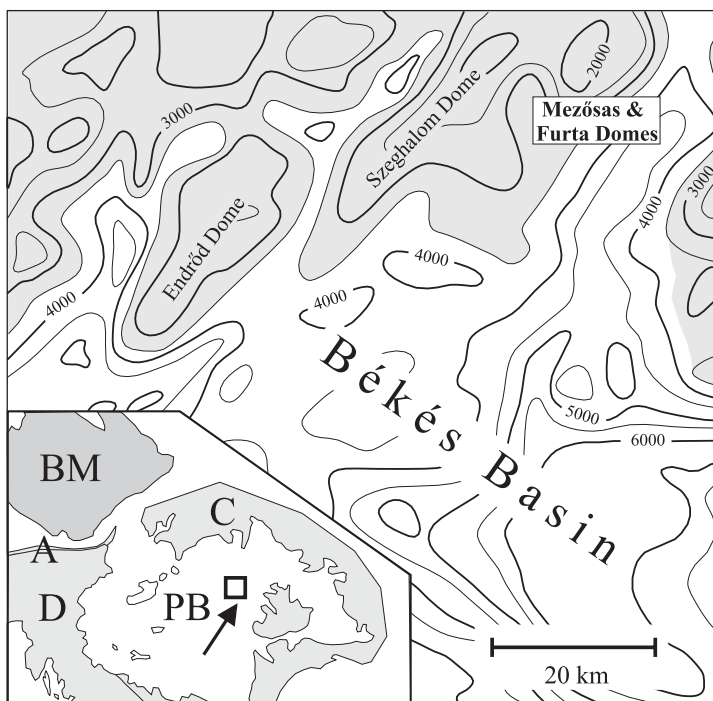
All rock units are characterized by a late normal fault system; the faults are filled with a regular mineral paragenesis of quartz, calcite and laumontite (Juhász et al. 2002). Quartz crystals contain diverse hydrocarbon and aqueous fluid inclusion assemblages (Schubert and M. Tóth 2003); while calcite encloses plant fragments of Neogene age (M. Tóth et al. 2003a).

Concerning the Mezősas-Furta Dome (MFD), the boreholes belonging to the Furta region are situated on the most elevated portion of the dome; Mezősas field occupies the southern slope of the same high (Fig. 2). The entire metamorphic complex has been considered petrologically homogeneous and so is classified within the same lithostratigraphic unit as previously (Balázs et al. 1986).

The petrology of the MFD was first outlined by Szili-Gyémánt (1986) and Balázs et al. (1986), who emphasized its petrologic affinity with the neighbouring metamorphic highs. They report gneiss, amphibolite, migmatite and granite as the main rock types. Unpublished reports give further details about the petrology and structural framework of the MFD. In the Mezősas region, within the dominating rock types (gneiss, amphibolite, migmatite) subtypes can also be distinguished, such as biotite gneiss, biotite-amphibole gneiss and garnet-bearing amphibolite. The intensely foliated rocks exhibit a schistosity of 20–60° dip; mylonitization is common. Although all previous studies confirm that in the Furta region gneiss and amphibolite are the principal components in the
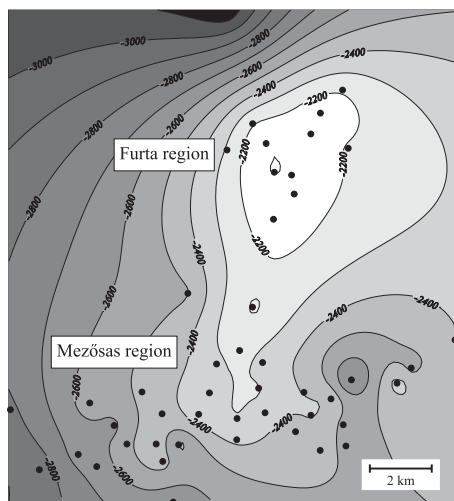
Fig. 2
Topographic map of the metamorphic Mezősas-Furta Dome. Dots show boreholes presented in the paper

basement, the spatial relationship of the two lithologies is still under debate. While according to the model of Szili-Gyémánt (1986) thin amphibolite layers are intercalated in the homogeneous gneiss body, Szepesházy (1971) assumes a homogeneous amphibolite injected by a dense network of granitoid (orthogneiss) dykes and sills. An unpublished report exhibits a homogeneous gneiss body overlain by a homogeneous amphibolite layer.

As shown by Pogácsás et al. (1989), Posgay and Szentgyörgyi (1991), Albu and Pápa (1992), Tari et al. (1992, 1999), and D. Lőrincz (1996) among others, the structural evolution of the Körös Complex during the Alpine orogeny and the following multiphase subsidence of the Pannonian Basin was rather complicated. Although some of these tectonic events certainly only had an effect on the cover formations, others also affected the basement, contributing to development of its heterogeneous structure. The Upper Cretaceous compression probably caused formation of a NE-verging nappe system. Sinistral transpression along the Middle Miocene Derecske–Biharnagybajom Line probably resulted in the formation of NW-dipping overthrusts along flat surfaces within the metamorphic basement. This inverse structure was further complicated by the north-south-trending horst-graben structure formed due to extension during the Badenian. The two deep trenches on the SW (Vésztő) and SE (Komádi-Mezősas) of the MFD were also formed due to such movements.

Samples and methodology

In the Mezősas region of the MFD, 35 wells penetrated the basement; at present 23 of them are available for petrologic study. There are 13 wells, which sampled the basement at different depth intervals; the others provide rock material from single cores only. In the Furta region, material of 11 of the total 12 wells is still available for petrologic study.

During microscopic studies and rock classification almost 300 thin sections were investigated, 165 of which represent the Mezősas region. The vast majority of the thin sections correspond to the collection of the Hungarian Oil and Gas Company (MOL Ltd.). At present, several samples are represented only by these slides; the original rock specimens cannot be found any more.

Representative electron microprobe measurements using an ARL-SEMQ 30 machine (15–20 keV, 30 nA, natural standards) were carried out at the Department of Applied Geosciences and Geophysics of the Montanuniversität Leoben (Austria) on selected samples in case of each identified rock unit.

Results

Petrography

The main rock types in the MFD region are different kinds of gneiss and amphibolite. Based on mineralogy and textural features they can be subdivided into the following main lithologies.

Orthogneiss

Orthogneiss in both localities of the MFD consists essentially of two feldspars, quartz and biotite; in some samples muscovite also occurs. The common accessory phases, zircon and apatite, are of euhedral shape (Fig. 3a, b). Because of the rather simple mineralogy, there is no obvious marker of the metamorphic peak assemblage. Titanite, epidote and white Mg-chlorite intercalated with biotite roughly specify the metamorphic conditions, whereas the total absence of sillimanite, even in the muscovite-rich samples, defines the upper thermal limit. Although based on its obvious gneissic structure, this rock type is clearly metamorphic in origin, with the common relic polygonal set of feldspar grains; in places, even quartz-feldspar aggregates within the common granoblastic texture recall an intrusive igneous protolith (Fig. 3c). Among others Vernon and Collins (1988) mention relic polygonal texture as the most important criterion for magmatic origin. K-feldspar often exhibits perthitic appearance, while plagioclase is at places myrmekitic (Fig. 3d). In both localities (Mezősas and Furta, respectively) orthogneiss contains different xenocrysts. The most common among them is garnet of diverse grain size, which is usually partially replaced by chlorite and carbonate minerals (Fig. 3e). In some samples, atoll-shaped garnet appears as well. Single, oriented amphibole grains usually have a resorbed rim. In most places, only tiny amphibole laths of identical orientation and optical features within the polygonal texture recall the existence of a previous, coherent grain (Fig. 3f). In places, large amphibole xenocrysts contain inclusions of clinopyroxene and garnet.

Also in the Furta region solid inclusion-bearing, resorbed feldspar porphyroblasts are set in the orthogneiss; the common inclusions are quartz, garnet, amphibole, rutile and ilmenite. The inclusion trails are oriented in each host feldspar grain, although in the case of different grains they exhibit significantly different orientations, even within the same specimen/thin section. The microstructure of this situation is sketched in Fig. 4.

Based on the above features orthogneiss samples can unequivocally be identified under the microscope. They can also be distinguished from other
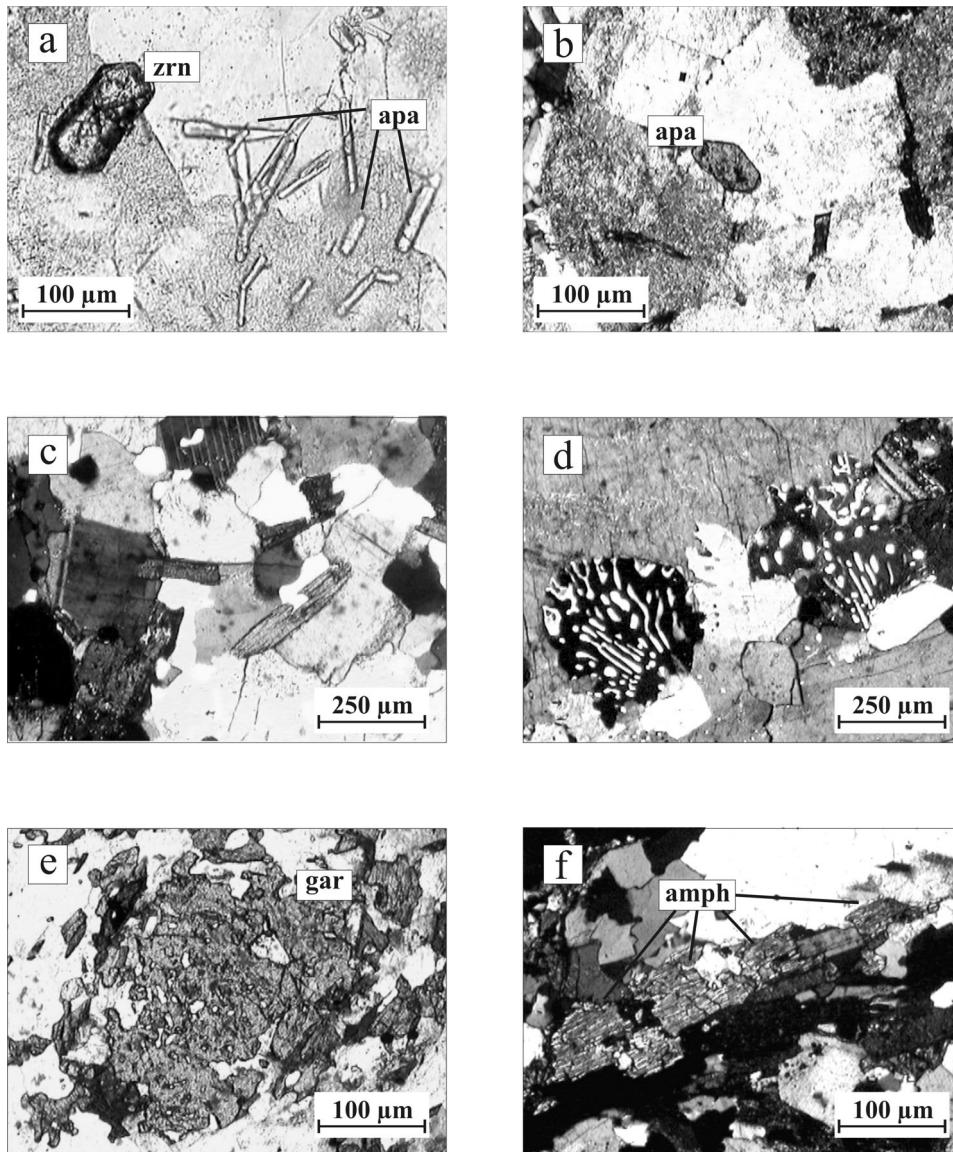
Fig. 3
Photomicrographs representing characteristic metamorphic textures from the MFD orthogneiss. Euhedral zircon (a, Fu-3, 1N) and apatite (b, Sas-Ny-7, +N) grains are widespread in the polygonal quartz-feldspar texture (c, Fu-12, +N). Plagioclase is commonly myrmekitic (d, Fu-11, +N). The most frequent xenocrysts in the orthogneiss are resorbed garnet (e, Fu-12, 1N) and segments of disintegrated amphibole laths (f, Fu-11, +N)
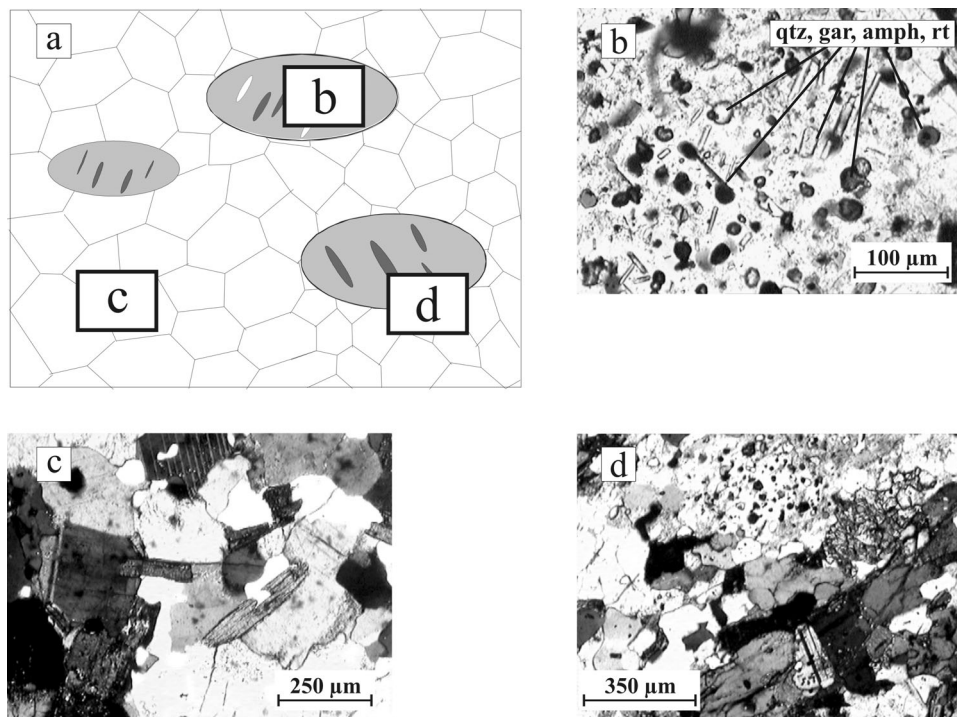
Fig. 4
Orthogneiss typically contains large, inclusion-rich feldspar grains situated in the polygonal quartz-feldspar matrix. On the sketch the spatial relationship of the characteristic textural elements is drawn (a), while photomicrographs (b, Fu-11, +N, c, Fu-12, +N, d, Fu-11, +N) demonstrate the inclusion-rich feldspar grain, the polygonal texture of the orthogneiss and the contact of these two, respectively

gneiss types of the MFD, although in some cases intensive late deformation conceals the diagnostic textural features entirely.

Mafic and ultramafic enclaves

Orthogneiss contains not only diverse xenocrysts but also a rather wide spectrum of xenoliths of mafic and ultramafic composition (Fig. 5a, b). The most common among these lithologies is garnet-bearing amphibolite (Fig. 5c), which itself can be subdivided into several subtypes. The compact amphibolite consists essentially of amphibole with little or no plagioclase content. Garnet either occurs as a matrix constituent or forms inclusions within large amphibole grains. Another common inclusion phase in amphibole grains is clinopyroxene, which systematically coexists with garnet (Fig. 5d). Occasionally olivine also forms inclusions in amphibole, while typical mesh-textured serpentine and magnetite aggregates after previous olivine are rather common in the amphibolite matrix (Fig. 5e–f). Rutile is a frequent inclusion mineral both in amphibole and in garnet.
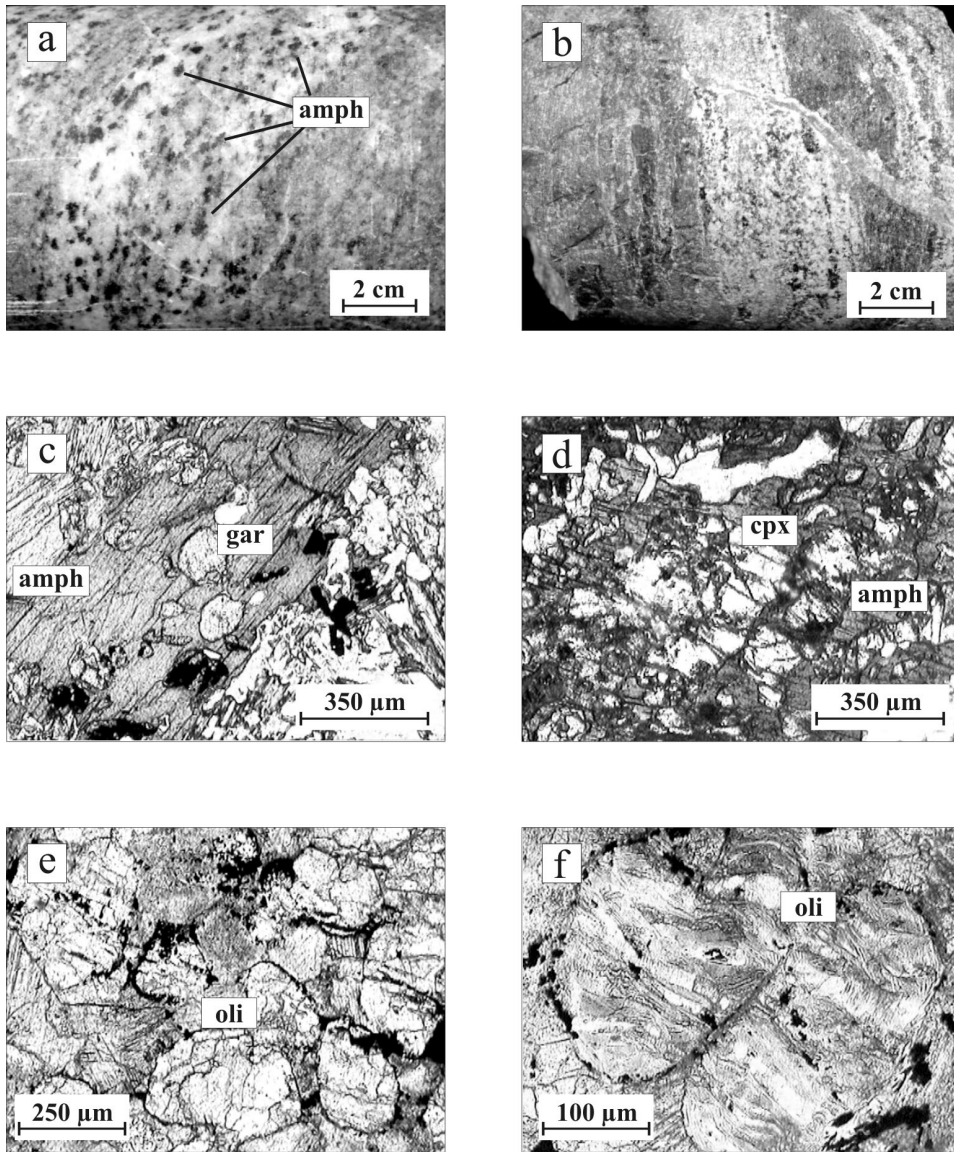
Fig. 5
Core and photomicrographs representing characteristic metamorphic textures from diverse xenoliths of the MFD orthogneiss. Many orthogneiss samples contain amphibole xenocrysts (a, Fu-12) and some of them also include xenoliths (b, Fu-8). The most typical xenolith is garnet-bearing amphibolite (c, Fu-10, 1N) occurring occasionally together with clinopyroxene (d, Fu-12, 1N). In a few samples relic olivine grains also appear in a serpentinized, carbonatized matrix (e–f, Fu-11 1N)

In plagioclase-rich amphibolite specimens large plagioclase crystals generally contain oriented inclusion trails of quartz, rutile and garnet. Amphibole, plagioclase (± olivine ± clinopyroxene, ± garnet) assemblages have also been preserved in highly altered calcite-rich rock samples.

A few xenoliths of actinolite schist, antophyllite schist and serpentinite mineralogy suggest clear ultramafic compositions (Fig. 6a, b).

There exists a gradual transition between massive mafic and ultramafic lenses and the orthogneiss containing the xenocrysts. Toward the orthogneiss, the amount of the large amphibole grains decreases, developing a resorbed, wiggly grain boundary.

Granite

In both parts of the studied MFD, granite plays only a minor role among the studied cores. It usually forms thin aplitic dykes crosscutting the massive orthogneiss body. This microgranite exhibits a non-deformed equigranular texture of K-feldspar, quartz, some plagioclase as well as a subordinate amount of mica grains. Based on textural features it can clearly be distinguished from the orthogneiss.

Amphibole-biotite gneiss

Amphibole-biotite gneiss is a typical rock type in the Mezősas region, while in the other area it was encountered only in the southernmost wells. Three main lithologies are classified in this category; in the whole rock sequence several cm-thick layers of biotite gneiss, amphibolite and amphibole-biotite gneiss interlock. In amphibolite, the common phases are the small-grained, in places even zoned green hornblende and plagioclase grains (Fig. 6c). Accessory phases are epidote, ilmenite and in some cases small, idiomorphic garnet; occasionally clinopyroxene grains of relic shape also appear in the amphibolite. Due to retrograde evolution of the amphibolite, prehnite (Fig. 6d), pumpellyite, titanite and green chlorite grew; hornblende is rimmed by secondary actinolite. In the gneiss sections quartz, K-feldspar and plagioclase dominate; the relevant mica is biotite, which is interlayered with white chlorite flakes. Some samples also contain small, syn-kinematic garnet grains. Amphibole-biotite gneiss always forms the transition from the massive amphibolite toward biotite gneiss.

Typical textural criteria of the orthogneiss are missing in these rock types; neither polygonal texture, nor myrmekitic plagioclase grains or resorbed xeno-crysts occur. Positive evidence is the lepidoblastic, nematoblastic texture typical for the amphibole-biotite gneiss as well as the occurrence of zoned amphibole and plagioclase grains. Nevertheless, similar mineralogy makes discrimination problematic in the case of highly deformed samples.
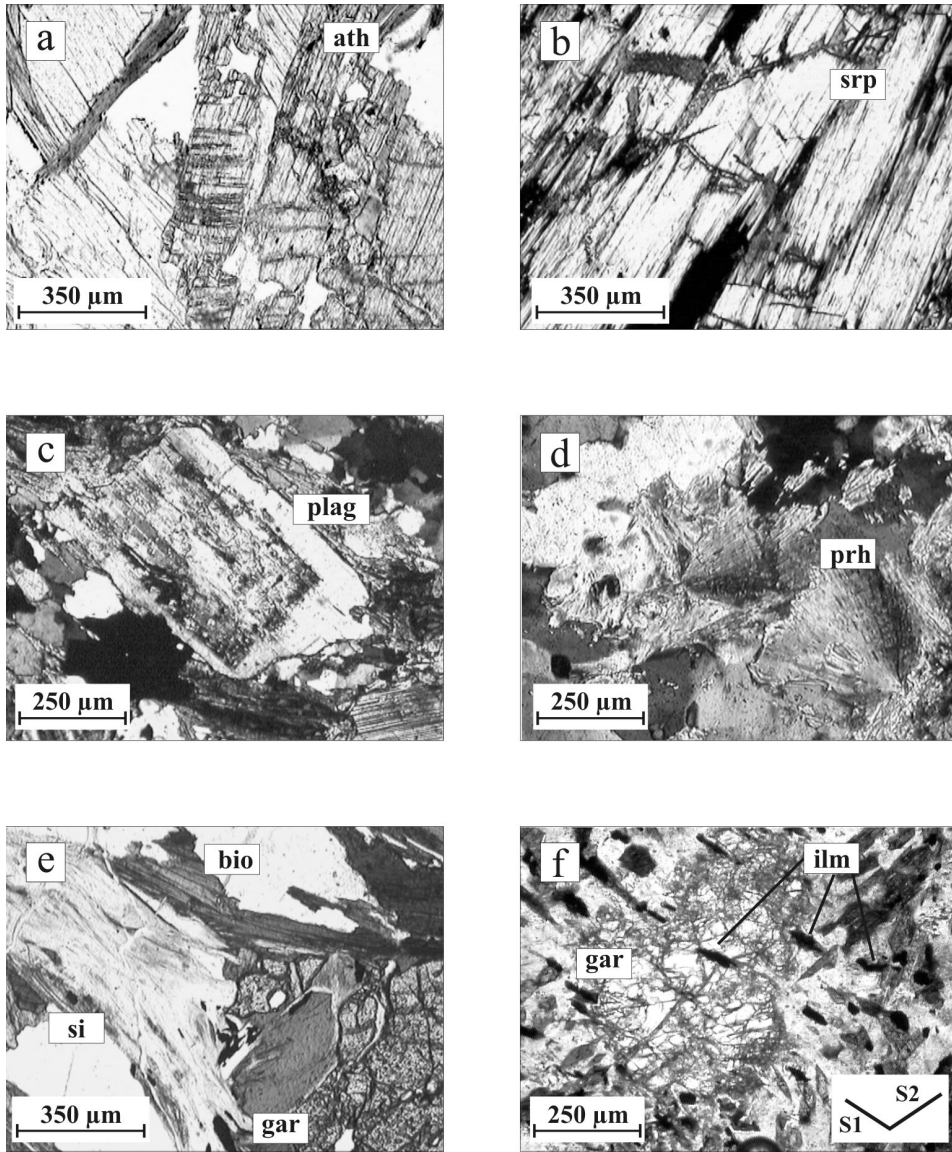
Fig. 6

Photomicrographs representing characteristic metamorphic textures from different MFD rock types. Some xenoliths reveal ultramafic composition, like antophyllite schist (a, Fu-10, 1N) or serpentinite (b, Fu-3, +N). In amphibole-biotite schist, zoned plagioclase crystals are widespread (c, Sas-Ny-12, +N). Due to late alteration processes, bunches of prehnite grew (d, Sas-Ny-2, +N). Sillimanite-biotite gneiss systematically contains resorbed garnet grains (e, Sas-1, +N). Garnet-bearing amphibolite is a typical intercalation in this rock type, in which ilmenite inclusion trails in garnet are oriented in a significantly different fashion from that shown by matrix amphiboles (f, Sas-DNy-1, +N)

Sillimanite-biotite gneiss

Sillimanite-biotite gneiss occurs exclusively in the Mezősas region, where it is the most characteristic rock type. It consists essentially of quartz, two feldspars and biotite; several samples also contain bunches of thin sillimanite needles (Fig. 6e). Muscovite is totally absent. Most samples include resorbed relic garnet grains (Fig. 6e) suggesting a pre-kinematic event, which is also confirmed by preserved schistosity of biotite. Common accessory phases are zircon, monazite and apatite. Discrimination of sillimanite-bearing samples from the other gneiss types is obvious; otherwise, in the case of sillimanite-free samples, it is rather problematic and in many cases remains obscure.

Garnet-bearing amphibolite

This massive, coarse-grained amphibolite variety appears exclusively in the Mezősas region. In addition to dark green amphibole and plagioclase it also contains large, resorbed garnet grains (Fig. 6f), which at places are entirely replaced by a fine-grained aggregate of plagioclase crystals. Based on the orientation of the rutile and ilmenite inclusion trails (S1) being significantly different from that shown by matrix amphiboles (S2), garnet is pre-kinematic. Taking into account these textural features, the rock type in question can unambiguously be discriminated from the amphibole-biotite gneiss variety.

Rock column

Although the relative spatial position of the lithologies detailed above is not exposed by each well, their vertical sequence is quite consistent in all studied situations (Fig. 7). As was suggested previously, mafic and ultramafic enclaves appear exclusively in tight connection with orthogneiss, which is the lowermost unit of the succession. Granite aplites penetrate only the orthogneiss unit. Sillimanite-biotite gneiss follows upward, in which intercalations of the massive garnet-bearing amphibolite are common. The uppermost unit in each studied case is amphibole-biotite gneiss. There is no

AG - Amphibole-biotite gneiss (biotite gneiss with amphibolite intercalations)

SG - Sillimanite-biotite gneiss, garnetiferous amphibolite

OG - Orthogneiss with mafic, ultramafic xenoliths

Granite aplites

Fig. 7
The idealized rock column of the MFD basement. In the uppermost position amphibole-biotite gneiss occurs, which is followed by the sillimanite-biotite gneiss unit along a tectonic contact. The lowermost unit is the xenolith-bearing orthogneiss
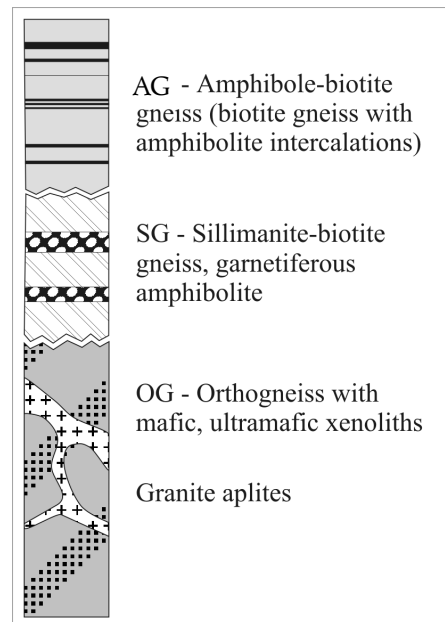
information available whether the boundaries between the three main units are structural or not; in fact the exact positions of the borders are unknown as well. In the following, the main lithologies are denoted by OG (for orthogneiss, xenoliths and granite), SG (for sillimanite-biotite gneiss and garnet-bearing amphibolite) and AG (for the varieties of the amphibole-biotite gneiss).

Deformation

A detailed study of post-metamorphic deformation textures, ductile and brittle elements as well as succeeding fracture systems may lead to better understanding of the structural evolution of the MFD and thus of the mechanism that caused the three blocks detailed above to become juxtaposed.

It was shown previously that SG is the only lithology, which suggests a clear polymetamorphic evolution; the other two rock units do not exhibit any evidence for such a complex history. All prograde metamorphic events together, without any further refinements, are symbolized by D0 in the following.

Several OG samples show clear textural evidence for post-peak metamorphic shearing. Recrystallized and strongly elongated quartz ribbons usually consist of subgrains with highly sutured grain boundary patterns (Fig. 8a); feldspar grains appear as curved twins (Fig. 8b). All these textural features, together with an advanced grain size reduction and locally developed secondary foliation of chlorite and sericite bands (S/C structures), point to the effect of mylonitic shearing in the orthogneiss unit (D1 event). OG samples show a late cataclastic texture as well (Fig. 8c); these cohesive microbreccia zones crosscut D1 mylonite. The fine-grained, cemented fault breccia usually encloses fractured pieces of the adjacent mylonite, clearly suggesting a D2 brittle overprint on the D1 event (Fig. 8d). The corresponding flat discontinuity surfaces in OG are coated by a thin chlorite and calcite film.

Both AG and SG samples are characterized by subhorizontal (0–15°) discontinuity surfaces covered by a thin (1–2 mm) chlorite and in places hematite coating. Slickensides and chatter marks in each case clearly record movement along reverse faults (Fig. 8e). Along these surfaces, biotite is altered to form chlorite and sericite; in AG samples secondary tremolite and prehnite also appear in the host rock (Fig. 6d). In those samples, which are poor in mica, a few cm-thick cohesive fault breccia and cataclasite zones develop that are separated from the undeformed and unaltered wall rock by sharp contact (Fig. 8f). The angular rock fragments do not show any orientation; the fault rock is entirely cemented by chlorite, quartz and pyrite (Fig. 9a). The milled rock pieces are frequently arranged in a sequence of pockets of monocline symmetry along the shear zones (Fig. 9b).

The entire rock complex, especially in its western part, is crosscut by a steep conjugated system of microfaults and joints (D3, Fig. 9c). Most of them are open and partially filled by a consistent series of fracture filling/sealing minerals:
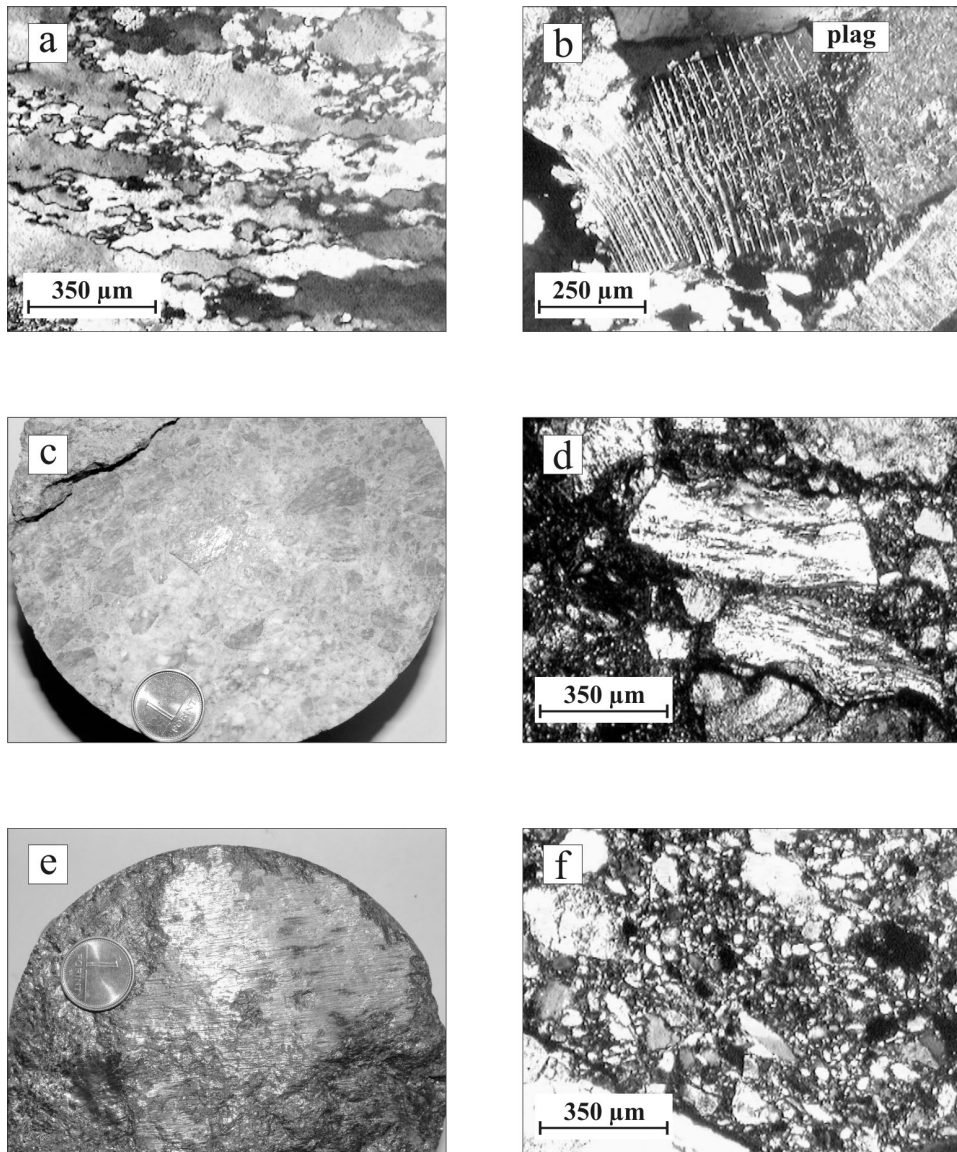
Fig. 8
Typical deformation features of certain MFD metamorphic rocks. In the orthogneiss elongated quartz ribbons (a, Sas-Ny-3, +N) and curved feldspar twins (b, Sas-Ny-3, +N) suggest the effect of shearing following peak metamorphism. In the late cataclasite zones of the orthogneiss (c, Sas-4) fragments of D1 mylonite are widespread (d, Sas-4, +N). In mica-rich samples slickensides suggest movement along low-angle reverse faults (e, Sas-16). The late cataclasite also formed in the amphibole-biotite gneiss unit (f, Sas-Ny-11)
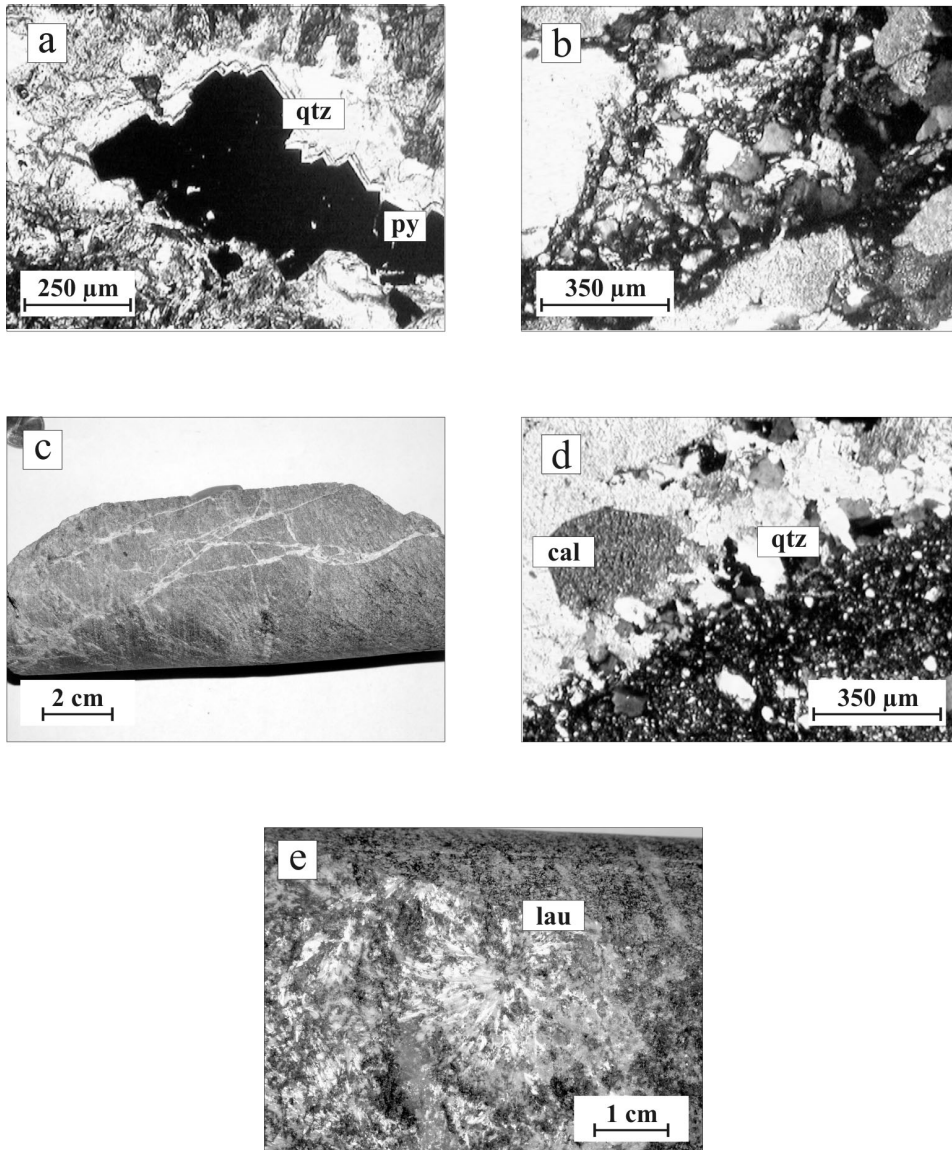
Fig. 9
Cataclasite is cemented by chlorite, quartz and pyrite (a, Sas-Ny-4): the milled rock is arranged into series of pockets of monocline symmetry (b, Sas-Ny-1, +N). The last brittle event caused formation of a steep conjugated system of microfaults and joints (c, Sas-Ny-9), which are filled by quartz, calcite (d, Sas-Ny-1, +N), and laumontite (e, Sas-DNy-1)

chlorite, quartz, calcite, laumontite (Fig. 9d, e). The latter phase occurs exclusively in the western part of the MFD, independent of the country rock lithology. In many places, calcite occurs as a pervasive phase causing an entire alteration of the host rock.

Considering all above observations, mylonitic deformation (D1) is common exclusively in the OG, while cataclastic reverse structures along flat surfaces (D2) as well as cemented normal faults (D3) are present in all three units.

Mineral chemistry

A comprehensive mineral chemical evaluation of all different rock types (including the wide spectrum of xenoliths) is beyond the scope of the present study. Moreover, several rock types are not available for a detailed petrologic study, because their ancient thin sections are all that is left of the original samples. That is why only a representative dataset is presented for the main lithologies.

In the studied orthogneiss sample (OG), clinopyroxene xenocrysts present a rather systematic composition. The crystals are not zoned; they all plot as Quad pyroxene, and based on the classification scheme of Morimoto (1989), each measured grain is a Fe-diopside or augite in composition. Si^{IV} is ~ 1.97; Al, Ti and Cr (Cr_2O_3 < 0.05%) are rather low. Pyroxene grains are usually overgrown by a hornblende rim of Al^{IV} ~ 1.5, Al^{VI} ~ 0.2, Na^{M4} ~ 0.2 using the $\Sigma FM=13$ scheme for calculation. Plagioclase in the matrix of the rock is around An_{30} (Table 1).

In the garnet-bearing sillimanite-biotite gneiss (SG) garnet is zoned with a core composition of $Alm_{78}Prp_4Grs_{12}Sps_6$ and a rim of $Alm_{62}Prp_7Grs_{20}Sps_{11}$. Garnet encloses quartz, plagioclase (An_{30-35}), and biotite inclusions in addition to tiny laths of an undetermined Al_2SiO_5 phase evidenced by its EDS spectrum. In the matrix of the sample, biotite and plagioclase are common constituents, while the stable Al_2SiO_5 phase is sillimanite. There is no muscovite present in the studied sample (Table 1). Representing the same unit, in a garnet-bearing amphibolite sample rutile-ilmenite-plagioclase inclusion assemblage in garnet (GRIPS) and matrix amphibole-plagioclase mineral pairs were measured for thermobarometry calculations. Garnet is around $Alm_{63}Prp_7Grs_{26}Sps_4$ with little or no zoning, ilmenite is Ilm_{95}, plagioclase as inclusion is around An_{30}, while as a matrix constituent it is lower in anorthite, being $\sim An_{15}$. Matrix amphibole is of Al^{IV} ~ 1.8, Al^{VI} ~ 0.7, Na^{M4} ~ 0.2, Na^A ~ 0.4 (Table 1).

Representing the amphibole-biotite gneiss unit (AG), an epidote-bearing amphibole-biotite gneiss sample was studied. Matrix hornblende is of Al^{IV} ~ 1.1, Al^{VI} ~ 0.6, Na^{M4} ~ 0.2, low in Ti; its secondary amphibole rim is tremolitic hornblende with Al^{IV} < 0.8, Al^{VI} ~ 0.0, Na^{M4} ~ 0.0. Plagioclase is An_{30}, in biotite Mg/(Fe+Mg) varies around 0.63 (Table 1).

Table 1
Representative compositions of significant mineral assemblages in the main rock units from the Mezősas-Furta Dome

	Cpx-OG	Cpx-OG	Cpx-OG	Pl1-OG	Amph1-OG	Pl2-OG	Amph2-OG	Gar-core-SG	Bio-incl-SG	Pl-incl-SG	Gar-rim-SG	Bio-matrix-SG	Pl-matrix-SG	Gar-GRIPS	Ilm-GRIPS	Pl-GRIPS	Gar-GRIPS	Ilm-GRIPS	Pl-GRIPS
SiO_2	52.67	52.09	51.93	62.16	41.68	67.25	42.71	37.37	33.95	60.94	42.99	37.13	64.87	37.25	0.00	66.3	38.60	0.02	66.54
TiO_2	0.06	0.04	0	0.07	1.93	0	1.25	0.07	1.16	0.04	0.00	2.30	0.00	0.17	53.38	0	0.08	52.31	0.00
Al_2O_3	1.39	1.39	0.26	23.33	10.43	20.18	7.70	19.04	18.54	23.02	17.00	17.10	21.09	21.97	0.00	22.12	21.90	0.00	23.13
FeO	12.78	14.65	15.77	0.24	21.49	0.3	24.91	37.26	24.78	0.09	29.47	24.55	0.21	22.68	43.41	0	29.02	44.21	0.26
MnO	0.61	0.84	1.39	0	0.62	0.03	0.73	1.79	0.27	0.00	6.25	0.35	0.03	4.89	2.85	0	1.47	2.64	0.00
MgO	10.01	9.98	9.7	0	7.51	0.13	7.55	3.26	6.56	0.00	2.36	7.00	0.00	0.90	0.00	0	3.66	0.01	0.00
CaO	20.76	21.05	19.47	4.78	10.85	4.14	11.00	2.33	0.00	6.77	0.83	0.00	4.72	10.88	0.15	2.57	7.06	0.06	2.06
Na_2O	0.84	0.77	0.16	9.58	1.63	9.44	1.19	0	0.21	7.89	0.22	0.20	9.17	0.00	0.00	8.46	0.00	0.00	5.51
K_2O	0	0.02	0.01	0.34	1.47	0.35	1.10	0.03	9.03	0.23	0.01	8.58	0.21	0.02	0.04	0.05	0.01	0.01	0.59
Total	99.12	100.83	98.72	100.52	97.61	101.84	98.13	101.15	94.50	98.99	99.13	97.21	100.30	98.75	99.82	99.5	101.79	99.26	98.09

	Amph1-matrix-GA	Pl1-matrix-GA	Amph2-matrix-GA	Amph1-AG	Pl1-AG	Amph2-AG	Pl2-AG	Amph3-AG	Bio1-AG	Bio2-AG	Epi1-AG	Epi2-AG
SiO_2	40.93	61.93	42.21	48.19	58.71	48.14	64.23	50.60	37.71	37.92	38.09	38.76
TiO_2	1.51	0.02	1.46	0.21	0.00	0.25	0.00	0.08	1.38	1.36	0.06	0.07
Al_2O_3	14.20	24.50	13.76	10.42	26.15	10.54	22.22	3.40	16.41	16.96	26.12	24.82
FeO	18.15	0.48	16.57	12.76	0.24	12.01	0.11	13.17	14.22	14.75	8.02	9.25
MnO	0.21	0.02	0.21	0.40	0.01	0.26	0.00	0.20	0.10	0.14	0.21	0.44
MgO	8.20	0.10	8.91	13.19	0.00	12.92	0.02	16.99	14.30	14.16	0.00	0.00
CaO	11.29	2.06	11.40	10.39	8.15	11.75	3.12	10.52	0.01	0.01	23.54	23.28
Na_2O	1.89	8.02	1.73	0.86	6.51	0.95	9.31	0.07	0.06	0.07	0.01	0.00
K_2O	1.05	2.17	1.02	0.24	0.07	0.23	0.05	0.12	10.06	9.41	0.01	0.01
Total	97.41	99.31	97.28	96.67	99.84	97.04	99.07	95.14	94.23	94.78	96.07	96.63

Thermobarometry

Relic clinopyroxene in the orthogneiss makes PT estimation for the xenocryst stability conditions possible. The low jadeite component as well as the negligible Cr-content points to low-pressure conditions. It is also confirmed by low Al^{VI} values of the amphibole (< 3 kbar using the estimation of Gerya et al. (1997). Using the single pyroxene enstatite-in-Cpx thermometer (Nimis and Taylor 2000), a coherent temperature of 810–830 °C can be obtained presuming 2–5 kbar. A similar temperature range (780–820 °C) can be calculated using the reaction edenite + quartz = tremolite + albite and the calibration of Holland and Blundy (1994) for amphibole xenocrysts and the surrounding plagioclase grains.

In the sillimanite gneiss unit two subsequent stages of the evolution can be evaluated. Biotite inclusions together with garnet core suggest a temperature of 730–750 °C (Bhattacharya et al. 1992), while using the GASP paragenesis and the Grs + 2Ky/Sil + Qtz = 3 An reaction, pressure is around 7.5–7.8 kbar. Using the same equilibria for matrix assemblages, temperature is 630–650 °C; pressure varies between 4–5 kbars. As muscovite does not appear either as an inclusion in the garnet or as a matrix phase, barometers based on the reactions Grs + Prp + Ms = 3An + Phl (and the identical for Fe end members) cannot be used.

In the studied garnet-bearing amphibolite, sample pressure estimation using inclusion compositions in the garnet and based on the approach of Bohlen and Liotta (1986) results in a fairly coherent K_D value in the case of the calibrated reaction Grs + 2Alm + Rt = 2Ilm + An + Qtz. There are, however, only limited possibilities for temperature estimation. Thermometry using Fe/Mn distribution between coexisting garnet and ilmenite (Pownceby et al. 1987a, b, 1991) seems an effective tool; Feenstra and Engi (1998), however, discuss in detail conspicuous problems concerning the thermodynamic background of this method and doubt the applicability of the method. In the present case, temperature data for ilmenite inclusions and host garnet vary between 800 and 2100 °C and so are unrealistic results. The fact that garnet is unzoned clearly suggests a high temperature diffusive homogenization, so pressure is calculated assuming a T between 600–800 °C and yields 10–12 kbar. For single matrix amphiboles, a temperature range of 640–680 °C and a pressure of 4 kbar was calculated by Gerya et al. (1997). For matrix amphibole – plagioclase pairs T ~ 670 °C is obtained at 5 kbar using the method of Blundy and Holland (1990).

For amphibole-plagioclase pairs in amphibole biotite gneiss (AG) similar results can be calculated by diverse approaches. The method of Holland and Blundy (1994) gives 550–570 °C, Gerya et al. (1997) yields 560 °C at 3–4 kbar, while Plyusnina (1982) results in 530 °C at 4 kbar.

Discussion and conclusions

The MFD metamorphic high consists essentially of three lithologic units of different origin and metamorphic evolution. At the highest structural position, a

metamorphosed volcano-sedimentary sequence is found, with the characteristic rock types of amphibolite, amphibole-biotite gneiss and biotite gneiss. The monometamorphic rock (T_{max}: 530–570 °C, PT_{max}: 3–4 kbar) usually preserved igneous relic grains of clinopyroxene and zoned plagioclase. Beneath the AG unit, separated by a cataclasite zone, a high-grade sillimanite-biotite paragneiss follows (SG). Resorbed garnet grains and the well-preserved pre-kinematic schistosity show its polymetamorphic evolution (S1: 730–750 °C, 7.5–7.8 kbar; S2: 630–650 °C, 4–5 kbar). In this zone polymetamorphic (S1: 600–800 °C, 10–12 kbar; S2: 640–680 °C, 4–5 kbar) garnet-bearing amphibolite intercalations are widespread.

At the deepest structural position an intensely deformed monometamorphic orthogneiss body can be found (OG). Its igneous origin is clearly proved by the common presence of idiomorphic accessory minerals (zircon and apatite), the myrmekitic plagioclase grains and the preserved polygonal quartz-feldspar textures. Its most characteristic feature is the usual appearance of mafic and ultramafic xenocrysts and xenoliths of different PT conditions.

Deformation patterns indicate a mylonitic deformation in the OG unit, while cataclastic reverse structures and cemented normal faults are present in all three units.

Spatial correlation

The lithologies that compose the MFD are quite similar to those making up the neighbouring SzD concerning both their petrography and deformation history. On these bases, one can compare structure and evolution of the two areas in order to obtain a better-developed scheme for a wider portion of the basement.

The northern slopes of both domes are dominated by orthogneiss of similar textural characteristics. In the SzD the protolith chemically was a volcanic arc granitoid intrusion of peraluminous character (M. Tóth et al. 2000). The metamorphic peak did not exceed 550–600 °C based on coexistent amphibole-plagioclase pairs; this datum was also confirmed by model calculations. These DOMINO/THERIAK (De Capitani 1994) PT estimations result in a T_{max} ~ 580–600 °C interval for the SzD orthogneiss (Zachar 2000; M. Tóth et al. 2000). Although there are no quantitative data concerning the metamorphic conditions of the OG at the MFD, because of the above similarities the PT data of the SzD are also considered valid in this case. A significant difference between the two localities appears in the amount and quality of mafic and ultramafic xenoliths and xenocrysts. While only a few xenocrysts have been observed in the SzD over tiny relic grains of amphibole and garnet, in the MFD – and especially in the case of the Furta area – a wide spectrum of xenoliths turned up. They typically suggest incompatible origin and metamorphic evolution. As a single example, the measured pyroxene and amphibole xenocrysts suggest igneous origin and equilibrium conditions at low pressure and 780–830 °C.

Previously Zachar and M. Tóth (2004) considered the orthogneiss rocks across the metamorphic basement of the Tisza Block to be similar to those described in Alaskan-type orogenic belts (e.g. Ochsner 1993; Zurbriggen 1996; Zurbriggen et al. 1997). These belts (also called subduction-accretionary complexes) are characterized by granitoid orthogneiss of peraluminous character and, as the most significant specialty, xenoliths of different PT conditions (Ochsner 1993). In these regions, during the emplacement of the original granitoid intrusion, the melt picked up pieces from the subduction mélange, which at present appear as xenocrysts and xenoliths in the orthogneiss. Based on the above characteristics the OG unit of the MFD seems to belong to the orthogneiss zone extending at least between the Jánoshalma Dome in the SW (Zachar and M. Tóth 2001; M. Tóth and Zachar 2003; Zachar and M. Tóth 2004) and the MFD in the NE. This model for the Furta and Mezősas gneiss complexes is just the opposite of that given by Szepesházy (1971), in which an enormous mafic body is assumed to have been injected by orthogneiss veins.

Mylonitic deformation of the orthogneiss in the SzD can be studied by deep wells over a thickness of 200 meters. Along this shear zone the normal orthogneiss changes to an intensely deformed mylonite under greenschist facies conditions along the retrograde part of the metamorphic pathway (Schubert and M. Tóth 2001). In the case of the MFD orthogneiss, mylonitic textures suggest the effect of an identical low-temperature, post-peak metamorphic deformation event, making the connection of the two orthogneiss localities very probable.

The appearance of granitoid veins is also very similar in the case of the SzD and MFD. These medium-grained, mica-poor samples are free of any metamorphic texture and are regarded as post-kinematic aplites.

Sillimanite-biotite gneiss is the most common rock type of the SzD of identical textural and mineralogical characteristics to that of MFD. In the case of the SzD previous calculations suggest a thermal peak of 640–700 °C based on Fe-Mg exchange in garnet-biotite pairs (M. Tóth et al. 2000) and DOMINO/THERIAK modeling, respectively (Zachar 2000). The lower thermal limit is defined by the sillimanite-in reaction connected to breakdown of muscovite. Pressure is in the range of 4–6 kbar. Both the two-phase evolution and the physical conditions of the last progressive event fit well into the two neighbouring areas. Garnet-bearing amphibolite intercalations with large, rutile inclusion-bearing, resorbed garnet grains are fairly common in both areas (M. Tóth 1994b). Their two-phase PT evolution is comparable to that obtained for the sillimanite-biotite gneiss, although the maximal pressure data differ significantly.

The lithology at the uppermost structural position in both highs is AG. In case of the SzD its protolith was back-arc basin tholeiitic basalt (M. Tóth 1994a). Based on the textural similarities as well as the identical structural situation, AG at the SzD and MFD suggest identical lithology. Based on amphibole-plagioclase thermometry its T_{max} varies around 580–620 °C in case of the SzD (M. Tóth et al. 2000) and is slightly lower at the MFD. It is coherent with common preservation

of relic igneous clinopyroxene and zoned plagioclase grains in the AG samples from the MFD, which also makes high-grade metamorphism impossible. Similarly to the MFD, in the SzD as well several AG samples contain a secondary actinolite rim around hornblende and a plagioclase rim of pure albite composition; together with newly grown prehnite and pumpellyite grains (M. Tóth 1994b). In the case of the SzD this latter phase exhibits an Al-pumpellyite composition of $Fe_2O_3 < 10\%$ (Liou 1979) characteristic under pumpellyite-actinolite subfacies conditions (Coombs et al. 1976). The increase of Fe^{3+} rimward (M. Tóth 1994b) clearly points to the retrograde origin of this assemblage.

Concerning post-metamorphic deformation history, the two neighbouring areas suggest a rather similar history. Greenschist-facies ductile deformation of the OG unit as well as cataclasite at the SG/AG border is characteristic in both cases (M. Tóth et al. 2000). Conjugated normal faults, and vein mineral paragenesis with pyrite, calcite, quartz and laumontite is typical throughout the entire SzD (Juhász et al. 2002). It is, however present exclusively in the westernmost part of the MFD.

Because petrography and evolution of most lithologies of the SzD have been recognized in the MFD, the similarity of the two basement highs seems to have been proved. Although only a few thermobarometric data on the main lithologies of the MFD are available at present, based on the described mineralogy, textures and the informative PT values, their similarity to those studied in the SzD appears valid.

Geologic map and sections over the Mezősas-Furta Dome

The most essential rock types and their evolution can be compared in the case of the two neighbouring crystalline highs (SzD and MFD, respectively). The vertical sequence of the lithologies is identical and the AG/SG border can be identified in both cases as well. OG becomes predominant in the northern part of both highs. A significant difference is, however, that while OG is present in the deepest wells in the Mezősas area, its existence cannot be proved directly for the southern part of the SzD.

Putting all lithological information on the map and sections of the MFD, clear NE–SW-oriented stripes of different rock types become evident. As an example, in studying the wells along the A-A' section as well as accepting the common vertical sequence of the three units OG, SG and AG, a series of overthrusts with NW-vergency appears obvious (Fig. 11a). Other sections parallel to that of A-A' exhibit similar geometry. Application of this model to the entire area suggests that the essential structure of the MFD can be explained by overthrusted AG/SG/OG triplexes (Fig. 10). This scenario is slightly modified on the southwestern end, where a series of NE-SW striking normal faults must be supposed (B-B' section, Fig. 11b). This horst-graben structure continues westward in the area of the SzD (M. Tóth et al. 2000), where the fracture filling mineral sequence is also identical to that of the western MFD.

Using microstructural data, M. Tóth et al. (2000) concluded that the OG-dominant northern realm of the SzD became juxtaposed to the southern block by Neogene strike-slip motions. Significant sinistral slip during the Lower Miocene was also improved by Posgay and Szentgyörgyi (1991) as well as Albu and Pápa (1992) evaluating seismic data. Nevertheless, in case of the MFD, geophysical data suggest a transpressional regime, which can be confirmed by the observed micro-textural features as well. Based on these data we conclude that in the MFD the common SG/OG border connects to this transpressional event. Whether OG unit is present below the
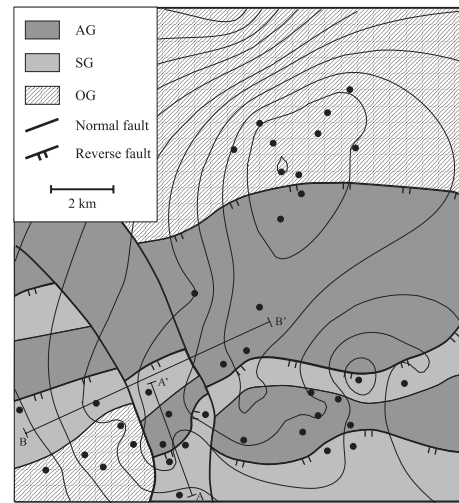

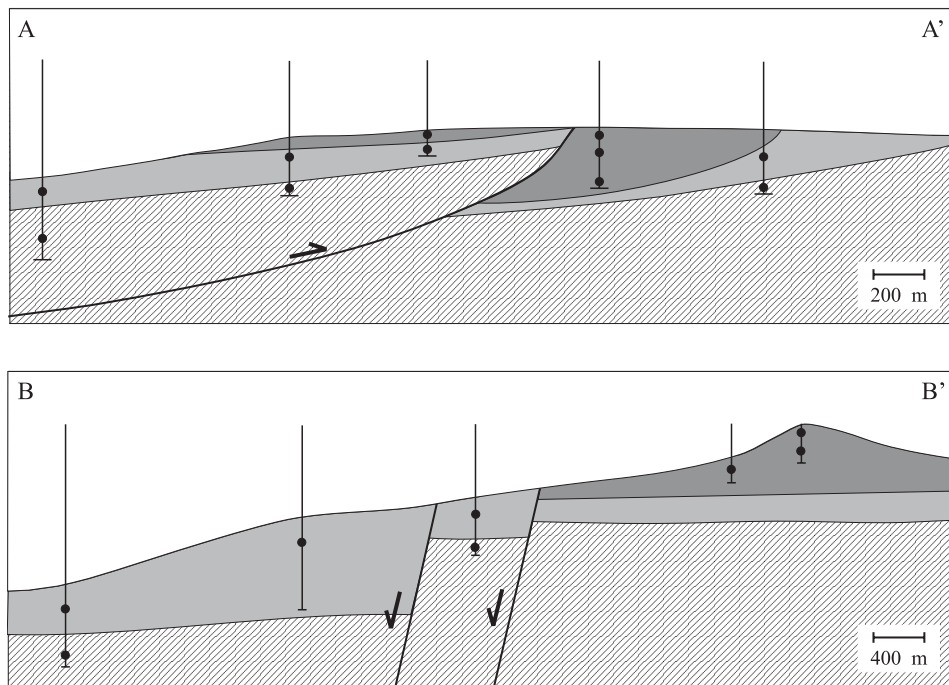Fig. 10
Geologic map of the MFD

Fig. 11
Representative geologic sections of the MFD. For details see text. The position of AA' and BB' sections are denoted on the map (Fig. 10)

SG rocks and therefore a SG/OG overthrust also exists in case of the SzD could only be proved by detailed geophysical methods.

The common cataclastic textures of AG samples as well as the retrograde mineral reactions identified (Fe/Al zoning in pumpellyite) suggest that the D2 compression was responsible for the development of the AG/SG border and for simultaneous alteration of metabasic rocks; during simultaneous cooling and hydration secondary actinolite, chlorite, prehnite and pumpellyite grew. On this basis the oversimplified structure of the MFD crystalline high can be sketched by a parautochtonous OG unit overthrusted by allochthonous AG/SG duplexes. In these latter packages the AG/SG border is of tectonic origin as well and is identical to that found in case of the Szeghalom Dome previously.

One can recognize that lithology, structure and evolution of the MFD are approximately identical to those known in the neighbouring Szeghalom Dome. In this way, following the multiphase Variscan metamorphism and post-Variscan exhumation, the present structure of the MFD must be the result of the over-lapping effects of the Cretaceous nappe tectonics and the various compressive, extensive and strike-slip events during the Neogene. As a result, SW–NE striking thrust zones separate the three lithological units, which exhibit a different metamorphic history. During the last tectonic event normal faults formed, which are characteristic in the westernmost part of the MFD.

Although the proposed model agrees with all petrologic and microstructural data, the probable metamorphic evolution as well as the available geophysical interpretations, it is based on a rather small set of information. That is why other spatial models may also exist, which, in some details, differ from ours.

Acknowledgements

References

Albu, I., A. Pápa 1992: Application of high-resolution seismics in studying reservoir characteristics of hydrocarbon deposits in Hungary. – Geophysics, 57/8, pp. 1068–1088.

Balázs, E., B. Cserepes-Meszéna, A. Nusszer, P. Szili-Gyémánt 1986: An attempt to correlate the metamorphic formations of the Great Hungarian Plain and the Transylvanian Central Mountains (Muntii Apuseni). – Acta Geologica Hungarica, 29/3–4, pp. 317–320.

Bhattacharya, A., L. Mohanty, A. Maji, S.K. Sen, M. Raith 1992: Non-ideal mixing in the phlogopite annite binary: constraints from experimental data on Mg-Fe partitioning and a reformulation of the biotite-garnet thermometer. – Contributions to Mineralogy and Petrology, 111, pp. 87–93.

Blundy, J.D., T.J.B. Holland 1990: Calcic amphibole equilibria and a new amphibole-plagioclase geothermometer. – Contributions to Mineralogy and Petrology, 104, pp. 208–224.

Bohlen, S.R., J.J. Liotta 1986: A barometer for garnet amphibolites and garnet granulites. – Journal of Petrology, 27, pp. 1025–1034.

Coombs, D.S., N. Nakamura, M. Vuagnat 1976: Pumpellyite-actinolite facies schists of the Taveyanne Formation near Loche, Valais, Switzerland. – Journal of Petrology, 17, pp. 440–471.

De Capitani, C. 1994: Gleichgewichts – Phasendiagramme: Theorie und Software. – Beihefte zum European Journal of Mineralogy 72, Jahrestagung der Deutschen Mineralogischen Gesellschaft, 6, 48 p.

D. Lőrincz, K. 1996: Feszültségtér történet meghatározása szeizmikus szelvényeken azonosított többfázisú tektonizmus alapján, a Szolnoki flis öv nyugati peremén (Determination of stress-field history on the basis of multiphase tectonism identified in seismic profiles in the Western part of the Szolnok flysh belt). – Magyar Geofizika, 37/4, pp. 228–246.

Feenstra, A., M. Engi 1998: An experimental study of the Fe-Mn exchange between garnet and ilmenite. – Contributions to Mineralogy and Petrology, 131, pp. 379–392.

Ferry, J.M., F.S. Spear 1978: Experimental calibration of the partitioning of the Fe and Mg between biotite and garnet. – Contributions to Mineralogy and Petrology, 66, pp. 113–117.

Gerya T.V., L.L. Perchuk, C. Triboulet, C. Audren, A.I. Sez'ko 1997: Petrology of the Tumanshet zonal metamorphic complex, Eastern Sayan. – Petrology, 5, pp. 503–533.

Holland, T.J.B., J.D. Blundy 1994: Non-ideal interactions in calcic amphiboles and their bearing on amphibole-plagioclase thermometry. – Contributions to Mineralogy and Petrology, 116, pp. 433–447.

Juhász, A., T. M. Tóth, K. Ramseyer, A. Matter 2002: Connected fluid evolution in fractured crystalline basement and overlying sediments, Pannonian Basin, SE Hungary. – Chemical Geology, 182, pp. 91–120.

Liou, J.G. 1979: Zeolite facies metamorphism of basaltic rocks from the East Taiwan Ophiolite. – American Mineralogist, 64, pp. 1–14.

M Tóth, T. 1994a: Geochemical character of amphibolites from Tisza Unit on the basis of trace elements. – Acta Mineralogica-Petrographica Szeged, 35, pp. 27–39.

M. Tóth, T. 1994: A Tiszai Egység amfibolitjainak premetamorf eredete és metamorfózisa Szeghalom környékén (Pre-metamorphic origin and metamorphic evolution of amphibolites of the Tisia Unit in the vicinity of Szeghalom). – PhD Thesis, Univ. Szeged, Hungary, 191 p. (In Hungarian.)

M. Tóth, T. 1997: Retrograded eclogite from the Kőrös Complex (Eastern Hungary): Records of a two-phase metamorphic evolution in the Tisia composite terrane. – Acta Miner. Petr. Szeged, 38, pp. 51–63.

M. Tóth, T., F. Schubert, J. Zachar 2000: Neogene exhumation of the Variscan Szeghalom Dome, Pannonian Basin, E. Hungary. – Geological Journal, 35, pp. 265–284..

M. Tóth, T., J. Zachar 2003: Evolution of the Déva orthogneiss (Tisza block, Hungary) and its geodynamic consequences. – Journ. of the Czech Geo. Soc. 48/1–2, pp. 127–128.

M. Tóth, T., M. Kedves, F. Schubert 2003a: Az Alföld metamorf aljzatának exhumációja a Szeghalom-dóm területén: Palinológiai bizonyítékok (Exhumation of the metamorphic basement of the Pannonian Basin (Szeghalom Dome, SE Hungary): Palynological constraints). – Földtani Közlöny, 133/4, pp. 547–562.

M. Tóth, T., Cs. Hollós, E. Szűcs, F. Schubert 2003b: Conceptual fracture network model of the crystalline basement of the Szeghalom Dome (Pannonian Basin, SE Hungary). – Acta Geologica Hungarica, 47/1, pp. 19–34.

Morimoto, N. 1989: Nomenclature of pyroxenes. – Canadian Mineralogist, 27, pp. 143–156.

Nimis, P., W.R. Taylor 2000: Single clinopyroxene thermobarometry for garnet peridotites. Part I. Calibration and testing of a Cr-in-Cpx barometer and enstatite-in-Cpx thermometer. – Contributions to Mineralogy and Petrology, 139, pp. 541–554.

Ochsner, A. 1993: U-Pb geochronology of the Upper Proterozoic-Lower Paleozoic geodynamic evolution in the Ossa-Morena Zone (SW Iberia): constraints on the timing of the Cadomian orogeny. – Unpubl. Ph.D. thesis, Diss. ETH. No. 10´392, ETH, Zürich, Switzerland.

Plyusnina, L.P. 1982: Geothermometry and geobarometry of plagioclase-hornblende bearing assemblages. – Contributions to Mineralogy and Petrology, 80, pp. 140–146.

Pogácsás, Gy., L. Lakatos, A. Barvitz, G. Vakarcs, Cs. Farkas 1989: Pliocén-quarter eltolódások a Nagyalföldön (fordítás). – Általános Földtani Szemle, 24, pp. 149–169.

Posgay, K., K. Szentgyörgyi 1991: A litoszférát harántoló oldaleltolódásos törésrendszer a Pannon-medence keleti részén (Strike-slip fault system crossing the lithosphere at the Eastern part of the Pannonian Basin). – Magyar Geofizika, 32/1–2, pp. 1–15. (In Hungarian with English abstract.)

Pownceby, M.I., V.J. Wall, H.St.C. O'Neill 1987a: Fe-Mn partitioning between garnet and ilmenite: experimental calibration and applications. – Contributions to Mineralogy and Petrology, 97, pp. 116–126.

Pownceby, M.I., V.J. Wall, H.St.C. O'Neill 1987b: Fe-Mn partitioning between garnet and ilmenite: experimental calibration and applications. Erratum. – Contributions to Mineralogy and Petrology, 97, p. 539.

Pownceby, M.I., V.J. Wall, H.St.C. O'Neill 1991: An experimental study of the effect of Caupon garnet-ilmenite Fe-Mn exchange equilibria. – American Mineralogist, 76, pp. 1580–1588.

Schubert, F., L.W. Diamond, T. M. Tóth. 2001: Hydrocarbon-bearing fluid inclusions in fracture-filling quartz from the crystalline basement of the Pannonian Basin (SE Hungary). – Memórias, 7, pp. 395–398.

Schubert, F., T. M. Tóth 2001: Structural evolution of mylonitized gneiss zone from the northern flank of the Szeghalom Dome (Pannonian Basin, SE Hungary). – Acta Mineralogica-Petrographica, 42, pp. 59–64.

Schubert, F., T. M. Tóth 2003: Successive, isothermal hydrocarbon migration events recorded by fluid inclusions in fracture-filling quartz in the Szeghalom Dome (Pannonian Basin, SE Hungary). – Acta Mineralogica-Petrographica, 44, pp. 9–17.

Szepesházy, K. 1971: Kőzettani adatok a Közép-Tiszántúl kristályos aljzatának ismeretéhez (Petrographical data on the crystalline basement of Middle-Tiszántúl region). – MÁFI Évi Jelentés 1971-ről: pp. 141–168. (In Hungarian.)

Szili-Gyémánt, P. 1986: Metamorphic formations in Tiszántúl: The Körös-Berettyó and the Álmosd Units. – Acta Geologica Hungarica, 29, pp. 305–316.

Tari, G., F. Horváth, J. Rumpler 1992: Styles of extension in the Pannonian Basin. – Tectonophysics, 208, pp. 203–219.

Tari, G., P. Dövényi, P., I. Dunkl, F. Horváth, L. Lenkey, M. Stefanescu, P. Szafián, T. Tóth 1999: Lithospheric structure of the Pannonian basin derived from seismic, gravity and geothermal data. – In: Durand, B., L. Jolivet, F. Horváth, M. Séranne, M. (Eds): The Mediterranean Basins: Tertiary Extension within the Alpine Orogen. Geological Society, London, Special Publications, 156, pp. 215–250.

Vernon, R.H., W.J.Collins 1988: Igneous microstructures in migmatites. – Geology, 16, pp. 1126–1129.

Zachar, J. 2000: Szeghalmi polimetamorf gneiszek PT modellezése. Szakdolgozat (PT modelling of polymetamorphic Szeghalom gneisses). – Thesis, Ásványtani, Geokémiai és Kőzettani Tanszék, Szegedi Tudományegyetem. (In Hungarian.)

Zachar, J., T. M. Tóth 2001: Myrmekite-bearing gneiss from the Szeghalom Dome (Pannonian Basin, SE Hungary) Part II.: Origin and spatial relationships. – Acta Min. Pet. Szeged, 42, pp. 39–43.

Zachar, J., T. M. Tóth 2004: Petrology of the metamorphic basement of the Tisza Block at the Jánoshalma high, S Hungary. – Acta Geol. Hungarica, 47/4, pp. 349–371.

Zurbriggen, R. 1996: Crustal genesis and uplift history of the Strona-Ceneri zone (Southern Alps): a combined petrologic, structural, geochemical, isotopic and paleomagnetic study. – Unpublished Ph.D. thesis, University of Bern.

Zurbriggen, R., L. Franz, M. Handy 1997: Pre-Variscan deformation, metamorphism and magmatism in the Strona-Ceneri Zone (southern Alps of northern Italy and southern Switzerland). – Schweizerische Mineralogische und Petrographische Mitteilungen, 77/3, pp. 361–380.